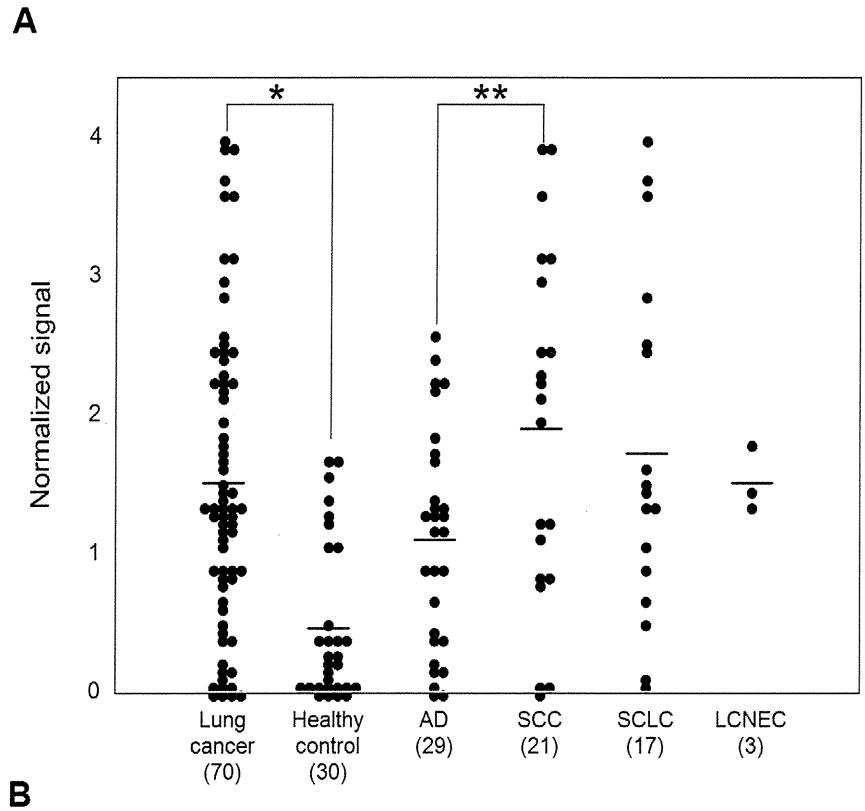

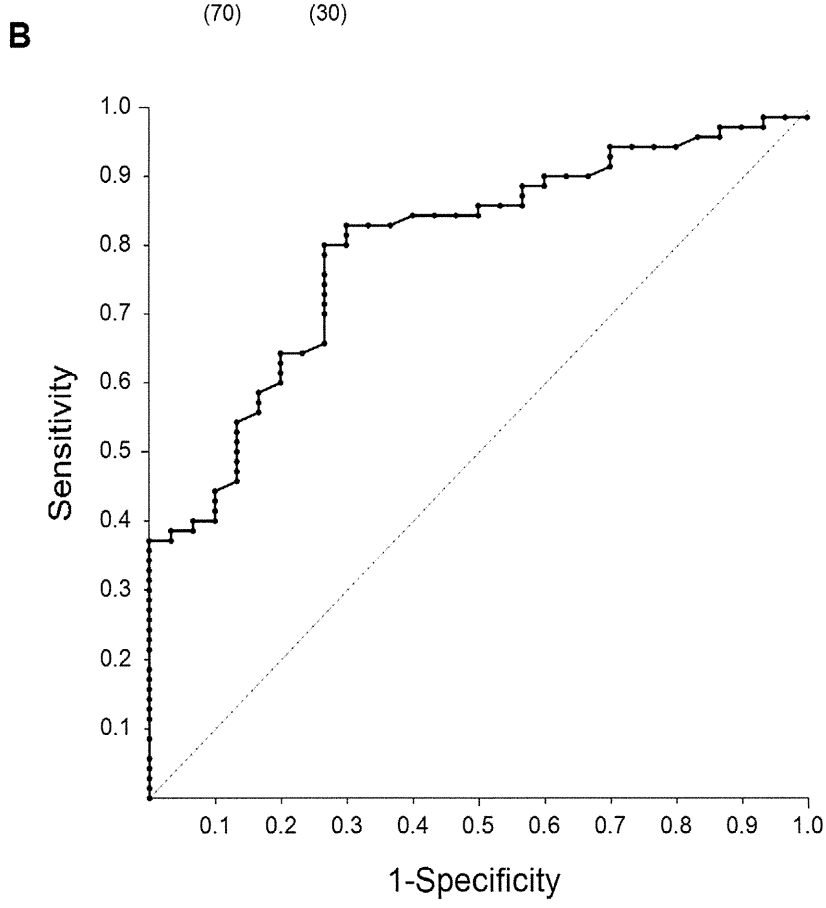

Figure 3. Serum CAXII levels in patients with lung cancer and healthy controls in the training set. Serum CAXII levels in patients with lung cancer and healthy controls. (A) The median CAXII level in the sera from healthy controls was 0.29, and that in sera from lung cancer patients was 1.52. Serum CAXII levels were significantly higher in lung cancer patients (*$P<0.001$). Furthermore, serum CAXII levels were higher in SCCs than ADs (**$P = 0.0381$). (B) Receiver-operating characteristic curve analysis of CAXII as a serum marker for lung cancer. The corresponding areas under the curves were 0.794 for CAXII. With a 70.0% specificity, the sensitivity of CAXII for lung cancer was 82.9%, at a cut-off value corresponding to 0.387.
doi:10.1371/journal.pone.0033952.g003

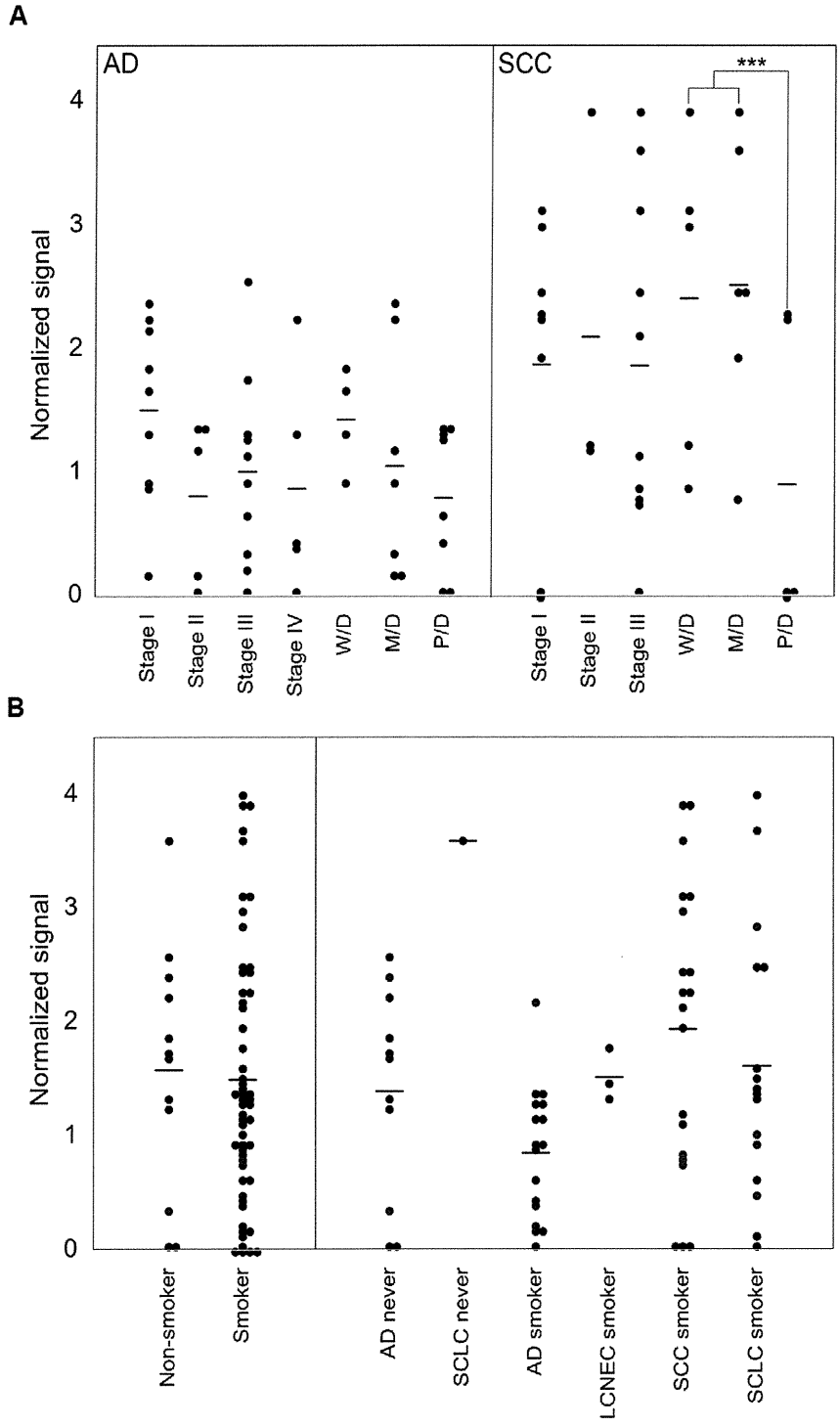

Figure 4. Correlation between serum CAXII levels and patients' clinicopathological characteristics. (A) CAXII levels in sera from patients with ADs and SCCs with a focus on the stage and differentiation. In SCCs, CAXII levels were significantly higher in well- and moderately differentiated tumors than in poorly differentiated ones (***P = 0.0272). In ADs, no significant difference based on the differentiation extent was detected. (B) Smoking history in lung cancer patients. The median CAXII level in the sera from non-smokers was 1.56, and that in smokers was 1.54, showing no significant difference.
doi:10.1371/journal.pone.0033952.g004

antibodies reacting with tumor-associated proteins localized in several intra-cellular compartments. The CAs constitute a family of ubiquitous enzymes with important roles in many physiological and pathological processes which reversely catalyse the conversion of CO_2+H_2O to HCO_3^- and H^+, contributing to regulation of the intracellular pH [6–11,19]. Several clinical studies have shown a clear relationship between high CAXII expression levels in tumor cells and a favorable prognosis.

Table 2. Serum CAXII levels in ADs and SCCs.

		Average value (AD)	Average value (SCC)
Stage	I	1.501	1.764
	II	0.704	2.093
	III	1.001	1.854
	IV	0.654	0.000
Tumor differentiation	Well	1.424	2.403
	Moderate	1.046	2.511
	Poor	0.727	0.742

doi:10.1371/journal.pone.0033952.t002

Watson *et al.* [12] reported that CAXII was expressed in 75% of invasive breast carcinoma cases, and was significantly associated with a lower histological grade ($P = 0.001$), positive estrogen receptor status ($P<0.01$), and negative epidermal growth factor receptor overexpression ($P<0.001$). Using univariate analysis, CAXII-positive tumors were associated with a lower relapse rate ($P = 0.04$) and a better OS ($P = 0.01$). On the other hand, although 98% of astrocytomas were immunohistochemically positive for CAXII, higher CAXII expression levels were correlated with a higher histological grade and a poorer patient outcome either by univariate ($P = 0.010$) or multivariate ($P = 0.039$) survival analysis [9].

An immunohistochemical study of the expression of CAXII in lung cancer was reported by Ilie *et al.* [13]. CAXII overexpression was observed in 105/555 cases, and was significantly associated with a better differentiation ($P = 0.015$) and SCC histological type ($P<0.001$). Furthermore, high CAXII expression was also significantly correlated with better overall and disease-specific survival. From our results, CAXII levels were higher in sera from SCC patients than ADs (Fig. 3 A). Also, they correlated more favorably with differentiation (Fig. 4 A). Integrating these results, CAXII may not only be a candidate tissue marker, but also a sero-diagnostic marker for lung cancer.

Although the association of CAXII expression and clinicopathologic factors and patient outcome in different tumors has been reported, to our knowledge, no study concerning the serum CAXII protein levels or its autoantibody levels in patients with tumors has been reported.

To confirm the possibility of CAXII as a sero-diagnostic marker, we measured its serum levels in patients with lung cancer and healthy controls. We demonstrated that the CAXII protein flowed out into the sera and its levels in patients with lung cancer were significantly higher than in healthy controls in both the training set ($P<0.0001$) and validation set ($P = 0.030$). It is possible that the gap in the P-value between the training set and validation set is caused by the fact that serum levels of CAXII of SCC patients were generally higher than those of patients with other

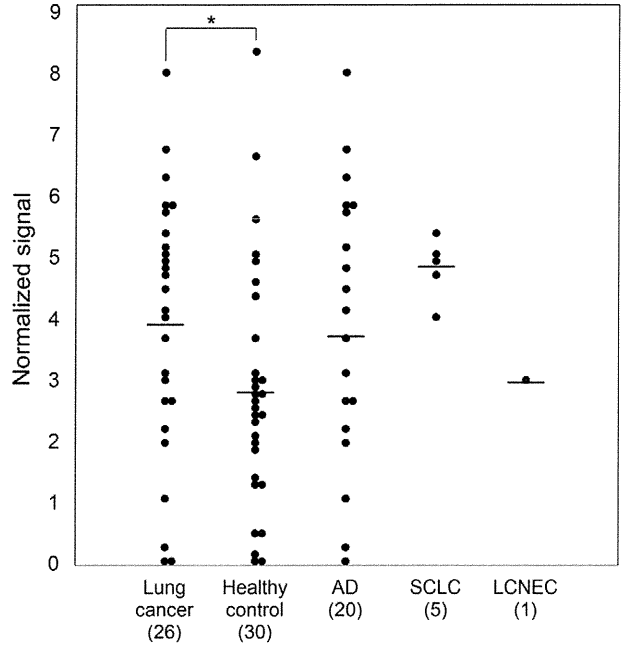

Figure 5. Serum CAXII levels in patients with lung cancer and healthy controls in the validation set. To confirm the utility of serum CAXII levels as a sero-diagnostic marker, 56 additional sera were analyzed by dot blot analysis as a validation study. The serum CAXII levels were also significantly higher in lung cancer patients than in healthy controls ($P = 0.030$). Relative values of serum CAXII levels ranged from 0.000 to 8.023 (median: 3.921) in lung cancer patients, but 0.000 to 8.331 (median: 2.806) in healthy controls.
doi:10.1371/journal.pone.0033952.g005

histologies, and the validation set included no SCC case. Taken together, the serum CAXII levels should be applicable markers discriminating lung cancer patients from healthy controls. Currently, CT scan or chest X-ray is the main method of lung cancer screening [21]. Mazzone et al. suggested that blood and breath tests should also be included for lung cancer screening, because they are both easy to perform and free of risks related to test administration [21,22]. In this study, we analyzed CAXII levels in sera from lung cancer patients and healthy controls using monoclonal antibody, and our results suggested that the serum CAXII level was a useful sero-diagnostic marker for lung cancer.

Author Contributions

Conceived and designed the experiments: MK TM Y. Sato. Performed the experiments: MK KY RN TM. Analyzed the data: MK TM SR. Contributed reagents/materials/analysis tools: SR YK NG SXJ MS AI Y. Satoh NM. Wrote the paper: MK TM RN Y. Sato.

References

1. Jemal A, Bray F, Center MM, Ferlay J, Ward E, et al. (2011) Global Cancer Statistics. CA Cancer J Clin 61: 69–90.
2. Jemal A, Siegel R, Xu J, Ward E (2010) Cancer statistics. CA Cancer J Clin 60: 277–300.
3. Patel JL, Erickson JA, Roberts Wl, Grenache DG (2010) Performance characteristics of an automated assay for the quantitation of CYFRA21-1 in human serum. Clin Biochem 43: 1449–1452.
4. Hirohashi S, Watanabe M, Shimosato Y, Sekine T (1984) Monoclonal antibody reactive with the sialyl-sugar residue of a high molecular weight glycoprotein in sera of cancer patients. Gann 75: 485–488.
5. Nagashio R, Sato Y, Matsumoto T, Kageyama T, Satoh Y, et al. (2010) Expression of RACK1 is a novel biomarker in pulmonary adenocarcinomas. Lung Cancer 69: 54–59.
6. Kivela A, Parkkila S, Saarnio J, Karttunen TJ, Kivela J, et al. (2000) Expression of a novel transmembrane carbonic anhydrase isozyme XII in normal human gut and colorectal tumors. Am J Pathol 156: 577–584.
7. Kivela AJ, Parkkila S, Saarnio J, Karttunen TJ, Kivela J, et al. (2005) Expression of von Hippel-Lindau tumor suppressor and tumor-associated carbonic anhydrases IX and XII in normal and neoplastic colorectal mucosa. World J Gastroenterol 11: 2616–2625.
8. Wykoff CC, Beasley N, Watson PH, Campo L, Chia SK, et al. (2001) Expression of the hypoxia-inducible and tumorassociated carbonic anhydrases in ductal carcinoma in situ of the breast. Am J Pathol 158: 1011–1019.
9. Haapasalo J, Hilvo M, Nordfors K, Haapasalo H, Parkkila S, et al. (2008) Identification of an alternatively spliced isoform of carbonic anhydrase XII in diffusely infiltrating astrocytic gliomas. Neuro Oncol 10: 131–138.

10. Hynninen P, Vaskivuo L, Saarnio J, Haapasalo H, Kivela J, et al. (2006) Expression of transmembrane carbonic anhydrases IX and XII in ovarian tumours. Histopathology 49: 594–602.
11. Parkkila S, Parkkila AK, Saarnio J, Kivela J, Karttunen TJ, et al. (2000) Expression of the membrane-associated carbonic anhydrase isozyme XII in the human kidney and renal tumors. J Histochem Cytochem 48: 1601–1608.
12. Watson PH, Chia SK, Wykoff CC, Han C, Leek RD, et al. (2003) Carbonic anhydrase XII is a marker of good prognosis in invasive breast carcinoma. Br J Cancer 88: 1065–1070.
13. Ilie MI, Hofman V, Ortholan C, Ammadi RE, Bonnetaud C, et al. (2010) Overexpression of carbonic anhydrase XII in tissues from resectable non-small cell lung cancers is a biomarker of good prognosis. Int J Cancer 128: 1614–1623.
14. Jiang SX, Kameya T, Asamura H, Umezawa A, Sato Y, et al. (2004) hASH1 expression is closely correlated with endocrine phenotype and differentiation extent in pulmonary neuroendocrine tumors. Mod Pathol 17: 222–229.
15. Sato Y, Mukai K, Watanbe S, Goto M, Shimosato Y (1986) The AMeX method. A simplified technique of tissue processing and paraffin embedding with improved preservation of antigens for immunostaining. Am J pathol 125: 431–435.
16. Laemmli UK (1970) Cleavage of structural proteins during the assembly of the head of bacteriophage T4. Nature 227: 680–685.
17. Nitori N, Ino Y, Nakanishi Y, Yamada T, Honda K, et al. (2005) Prognostic significance of tissue factor in pancreatic ductal adenocarcinoma. Clin Cancer Res 11: 2531–2539.
18. Goshima N, Kawamura Y, Fukumoto A, Miura A, Honma R, et al. (2008) Human protein factory for converting the transcriptome into an in vitro-expressed proteome. Nature Methods 5: 1011–1017.
19. Akishima-Fukusawa Y, Ino Y, Nakanishi Y, Miura A, Moriya Y, et al. (2010) Significance of PGP9.5 expression in cancer-associated fibroblasts for prognosis of colorectal carcinoma. Am J Clin Pathol 134: 71–79.
20. Battke C, Kremmer E, Mysliwietz J, Gondi G, Dumitru C, et al. (2011) Generation and characterization of the first inhibitory antibody targeting tumor-associated carbonic anhydrase XII. Cancer Immunol Immunother 60: 649–658.
21. Mazzone PJ (2010) Lung cancer screening: an update, discussion, and look ahead. Curr Oncol Rep 12: 226–234.
22. Mazzone PJ, Mekbail T (2007) Lung cancer screening. Curr Oncol Rep 9: 265–274.

FEBS Letters xxx (2012) xxx–xxx

FEBS Letters

journal homepage: www.FEBSLetters.org

Expression screening of 17q12–21 amplicon reveals GRB7 as an ERBB2-dependent oncogene

Makoto Saito [a], Yukiko Kato [a], Emi Ito [b], Jiro Fujimoto [a], Kosuke Ishikawa [a,c], Ayano Doi [a], Kentaro Kumazawa [a], Atsuka Matsui [a], Shiori Takebe [a], Takaomi Ishida [a], Sakura Azuma [a], Hiromi Mochizuki [c], Yoshifumi Kawamura [c], Yuka Yanagisawa [b,d], Reiko Honma [b,d], Jun-ichi Imai [b], Hirokazu Ohbayashi [e], Naoki Goshima [f], Kentaro Semba [a,*], Shinya Watanabe [b]

[a] Department of Life Science and Medical Bioscience, School of Advanced Science and Engineering, Waseda University, 2-2 Wakamatsu-cho, Shinjuku-ku, Tokyo 162-8480, Japan
[b] Department of Clinical Genomics, Translational Research Center (Tokyo Branch), Fukushima Medical University, Shibuya-ku, Tokyo 151-0051, Japan
[c] Japan Biological Informatics Consortium (JBiC), 2-45 Aomi, Koto-ku, Tokyo 135-8073, Japan
[d] Nippon Gene, Co., Ltd., Kandanishiki-cho, Chiyoda-ku, Tokyo 101-0054, Japan
[e] Nichirei Biosciences Inc., Biosciences Research & Development Center, 1-52-14 Kumegawa-cho, Higashimurayama-shi, Tokyo 189-0003, Japan
[f] Biomedicinal Information Research Center (BIRC), National Institute of Advanced Industrial Science and Technology (AIST), 2-42 Aomi, Koto-ku, Tokyo 135-0064, Japan

ARTICLE INFO

Article history:
Received 10 April 2012
Revised 30 April 2012
Accepted 2 May 2012
Available online xxxx

Edited by Takashi Gojobori

Keywords:
Gene amplification
Expression screening
Tumorigenesis
GRB7
ERBB2

ABSTRACT

Gene amplification is a major genetic alteration in human cancers. Amplicons, amplified genomic regions, are believed to contain "driver" genes responsible for tumorigenesis. However, the significance of co-amplified genes has not been extensively studied. We have established an integrated analysis system of amplicons using retrovirus-mediated gene transfer coupled with a human full-length cDNA set. Applying this system to 17q12–21 amplicon observed in breast cancer, we identified GRB7 as a context-dependent oncogene, which modulates the ERBB2 signaling pathway through enhanced phosphorylation of ERBB2 and Akt. Our work provides an insight into the biological significance of gene amplification in human cancers.

1. Introduction

DNA amplification is a major genetic alteration contributing to oncogenesis [1]. Historically, some proto-oncogenes identified as cellular counterparts of retroviral oncogenes were found to be amplified in human cancers. Thus, it is thought that unidentified proto-oncogenes exist in amplified genomic regions called "amplicons", and amplified proto-oncogenes express large amount of proteins, leading to oncogenesis. We previously constructed gene expression maps of chromosomes in human breast cancer cell lines and extracted six novel amplicons [2]. Nevertheless, it is not easy to identify such proto-oncogenes because amplification events often include multiple genes, and because more information is required, including precise mapping of amplified regions in multiple cancers and deduced function of each gene. A few findings provided the significance of co-amplified genes except specific oncogenes in the amplicon in terms of cancer cell phenotypes. In non-small-cell lung cancer, for instance, co-amplification of *TTF-1* and *NKX2-8* in the 14q13.3 amplicon renders cancer cells resistance to cisplatin [3]. However, the biological significance of co-amplification for oncogenesis has not been validated extensively.

In this study, we focused on the functions of co-amplified genes localized in the 17q12–21 amplicon containing *ERBB2* as a driver gene [4]. The *ERBB2* amplicon is observed in 25% of breast cancers, and also in ovarian, gastric and esophagus cancers [5]. Clinicopathological data indicate that ERBB2 expression is a poor prognostic factor [6]. Furthermore, an active *ErbB2* mutant called *neu* oncogene causes cellular transformation of NIH3T3 cells [7] and breast cancer in trans-

Abbreviations: GRB7, growth factor receptor-bound protein 7; ERBB2, v-erb-b2 erythroblastic leukemia viral oncogene homolog; MMTV, mouse mammary tumor virus; CMV, cytomegalovirus; MAPK, mitogen-activated protein kinase; MEK, MAPK extracellular signal-regulated kinase; ERK, extracellular signal-regulated kinase; IGF1, insulin-like growth factor-1

* Corresponding author. Fax: +81 3 5369 7320.
E-mail address: ksemba@waseda.jp (K. Semba).

0014-5793/$36.00 © 2012 Federation of European Biochemical Societies. Published by Elsevier B.V. All rights reserved.
http://dx.doi.org/10.1016/j.febslet.2012.05.003

Please cite this article in press as: Saito, M., et al. Expression screening of 17q12–21 amplicon reveals GRB7 as an ERBB2-dependent oncogene. FEBS Lett. (2012), http://dx.doi.org/10.1016/j.febslet.2012.05.003

genic mice expressing *neu* oncogene under the control of MMTV promoter [8]. These results support the idea that *ERBB2* functions as a driver gene for oncogenesis when mutated or overexpressed.

To examine the function of co-amplified genes in the *ERBB2* amplicon, we tested these genes for enhancement of ERBB2 cellular transforming activity. For this purpose, we introduced a human wild-type (WT) *ERBB2* expression vector into NIH3T3 cells and established "non-transformed" cells moderately expressing ERBB2 under the CMV promoter. Then, human full-length cDNAs of co-amplified genes were retrovirally introduced into ERBB2-expressing NIH3T3 cells, and the transforming activity was assessed by focus formation assays. Our screening system ensures multiple expression of complete proteins in cells, thereby enabling the examination of combinations of co-amplified genes in the *ERBB2* amplicon.

Here, we show *GRB7* gene, which is located about 10 kb from *ERBB2* locus and is frequently co-amplified with *ERBB2*, caused efficient transformation of NIH3T3 in concert with *ERBB2*; this ERBB2-dependent transforming activity was specific for GRB7 among the GRB7 family proteins. This was consistent with the observation that phosphorylation of ERBB2 was increased when GRB7 was expressed, but not other GRB7 family proteins. Importantly, phosphorylation of Akt at Thr308 and Ser473 was upregulated when both ERBB2 and GRB7 were expressed. We further examined the transforming activity of a series of GRB7 mutants, and showed that a BPS region deletion mutant of GRB7 is a potent activator of ERBB2 and Akt, while the transforming activities of other domain deletion mutants are severely impaired.

Our model of collaborative transformation by ERBB2 and GRB7 proposes that GRB7 is a cytoplasmic activator and adaptor of ERBB2, enhances ERBB2 phosphorylation, and connects ERBB2 to Akt. Our analysis also highlights the biological significance of gene amplification in terms of simultaneous overexpression of a driver gene and "supporter" genes.

2. Materials and methods

2.1. DNA constructs and antibodies

To construct an ERBB2 expression vector, human ERBB2 (RefSeq: NM_004448) cDNA was inserted in pQCXIN retroviral vector (Clontech, Mountain View, CA). Human full-length cDNAs were obtained from the human proteome expression resource (HuPEX) [9], and cloned into pMXs retroviral vector [10] using the Gateway Cloning system (Life Technologies, Carlsbad, CA) with or without N-terminal FLAG epitope tag. Venus fluorescent protein [11] was used as a control. Primary antibodies were as follows: anti-α-tubulin DM1A (Sigma, St. Louis, MO), anti-FLAG M2 (Sigma), anti-ERBB2 (SV2-61γ, Nichirei Bioscience, Japan), anti-HER2/ErbB2 (#2242, Cell Signaling Technology (CST), Danvers, MA), anti-Phospho-HER2/ErbB2 (Tyr877) (CST#2241), anti-Phospho-HER2/ErbB2 (Tyr1221/1222) (CST#2243), anti-Phospho-HER2/ErbB2 (Tyr1248) (CST#2247), anti-Erk1/2 (CST#4695), anti-Phospho-Erk1/2 (#4370), anti-Phospho-MEK1/2 (CST#9154), anti-Akt (pan) (#4691), anti-Phospho-Akt (Thr308) (CST#2965), anti-Phospho-Akt (Ser473) (CST#4060), and anti-Phosphotyrosine 4G10 (Millipore, Billerica, MA). Secondary antibodies for western blotting were purchased from GE Healthcare (Piscataway, NJ).

2.2. Cell culture

NIH3T3 cells were obtained from RIKEN Cell Bank (Tsukuba, Japan) and cultured in DMEM supplemented with 5% heat-inactivated calf serum, 100 U/ml penicillin, and 100 μg/ml streptomycin at 37 °C and 5% CO_2. 3T3-ERBB2 cells were established by retroviral infection of pQCXIN-ERBB2 and selection with 1 mg/ml G418. Plat-E packaging cells were obtained from T. Kitamura (Institute of Medical Science, University of Tokyo), and cultured

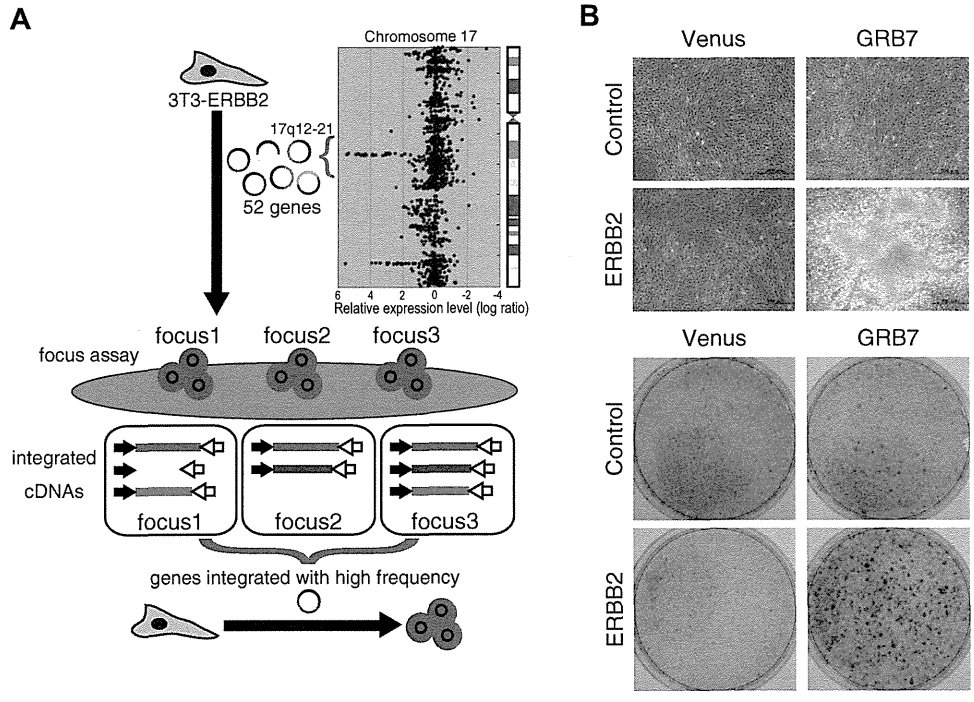

Fig. 1. ERBB2-dependent transforming activity of GRB7. (A) A scheme of oncogene-screening of ERBB2 amplicon. (B) Focus formation assays with ERBB2 and GRB7. 3T3-ERBB2 were infected with GRB7, and cultured for 17 days (upper). Scale bar, 500 μm. Cells were fixed and stained with crystal violet (lower). Venus fluorescent protein was used as a control. Volume of virus stock used in this experiment was 125 μl.

Please cite this article in press as: Saito, M., et al. Expression screening of 17q12–21 amplicon reveals GRB7 as an ERBB2-dependent oncogene. FEBS Lett. (2012), http://dx.doi.org/10.1016/j.febslet.2012.05.003

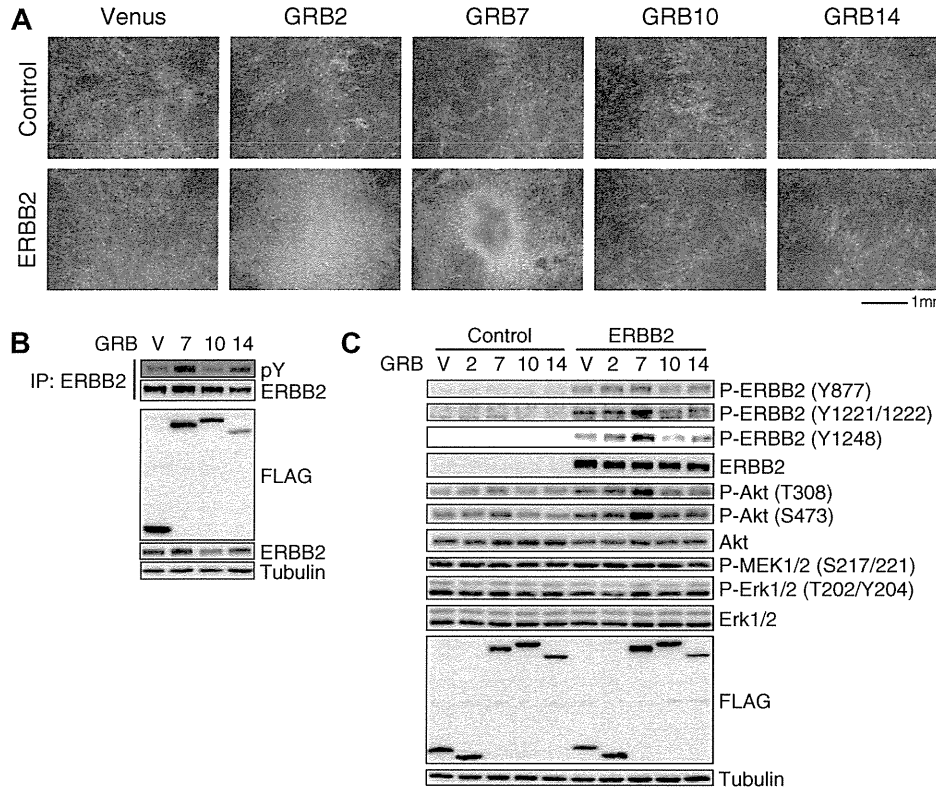

Fig. 2. ERBB2-dependent Akt activation and transformation by GRB7. (A) Focus formation assays with GRB proteins and ERBB2. 3T3-ERBB2 were infected with each GRB7 family protein or GRB2, and cultured for 20 days. Scale bar, 1 mm. (B) Phosphorylation status of ERBB2 in GRB7 family-expressing cells. ERBB2 immunoprecipitates prepared from GRB7 family-expressing cells were analyzed by anti-phosphotyrosine antibody. (C) Effect of expression of ERBB2 with GRB proteins. Phosphorylation status of ERBB2 and components of MAPK and Akt pathways were analyzed by phosphorylation-specific antibodies. Distinct amount of virus stock was used as follows: Venus (30 μl), GRB2 (480 μl), GRB7 (90 μl), GRB10 (360 μl), GRB14 (480 μl) for control NIH3T3, and Venus (20 μl), GRB2 (360 μl), GRB7 (60 μl), GRB10 (240 μl), GRB14 (360 μl) for 3T3-ERBB2.

in DMEM supplemented with 10% heat-inactivated FBS, penicillin, and streptomycin, as above.

2.3. Retroviral packaging

Plat-E cells were seeded into 6-cm culture dishes at a density of 1.0×10^6 and transfected with 4 μg of retroviral plasmids mixed with 10 μl of Lipofectamine 2000 reagent (Life Technologies). One day after transfection, the culture supernatant was replaced with NIH3T3 media. The following day, culture supernatant was harvested and centrifuged to remove cell debris, then stored at −80 °C as virus stock.

2.4. Focus formation assays

NIH3T3 cells were seeded into 12-well culture plates at a concentration of 5.0×10^4 and the following day, the cells were infected with 1 ml of appropriately diluted virus stock containing 8 μg/ml polybrene. To carefully adjust the expression level of each protein, distinct amount of virus stock were used. The next day, cells were seeded into 10-cm culture dishes and cultured for several days. Then, infected cells (1.0×10^5) were seeded again into 10-cm culture dishes and maintained for 2–3 weeks with medium change every 2 days. Cell foci were stained with 0.05% crystal violet and counted.

2.5. Recovery of cDNAs from NIH3T3 transformants

Transformed NIH3T3 cells were picked from each focus and cultured to isolate genomic DNA. cDNAs inserted into genome were amplified with a pair of primers for pMX vector (pMXs-s1811: GACGGCATCGCAGCTTGGATA and pMXs-AS3200: TTATCGTCGACCACTGTGCTG) and KOD FX polymerase (Toyobo, Japan) for 30 cycles of 98 °C for 10 s, 55 °C for 15 s, and 68 °C for 2 min, and subcloned into pBluescript SK(−) (Agilent Technologies, Santa Clara, CA). Two hundred and thirteen informative sequences were obtained by an Applied Biosystems 3130 genetic analyzer (Life Technologies).

2.6. Constructs of GRB7 mutants

To construct expression vectors for GRB7 mutants, pMXs-FLAG-GRB7 plasmid was amplified with an appropriate set of primers, then the PCR product was self-ligated to obtain a mutated plasmid [12].

2.7. Western blotting and immunoprecipitation

Cells were rinsed in ice-cold PBS and lysed in RIPA buffer (10 mM Tris–HCl, pH8.0, 150 mM NaCl, 1 mM EDTA, 1% NP-40, 0.1% sodium deoxycholate, 0.1% SDS, 1 mM Na_3VO_4, 10 mM NaF, 17.5 mM β-glycerophosphate, and 1 mM PMSF) for analysis of total cell lysates, or Triton lysis buffer (50 mM Tris–HCl, pH 8.0, 135 mM NaCl, 1 mM EDTA, 1% TritonX-100, 10% glycerol, 1 mM Na_3VO_4, 10 mM NaF, and 1 mM PMSF) for immunoprecipitation. Protein amounts used in Figs. 2B and 4 were 225 and 500 μg, respectively. Protein lysates were incubated with 2 μg anti-ERBB2 (SV2-61γ) for 1 h at 4 °C, and immunoprecipitated with 20 μl of protein A-Se-

Please cite this article in press as: Saito, M., et al. Expression screening of 17q12–21 amplicon reveals GRB7 as an ERBB2-dependent oncogene. FEBS Lett. (2012), http://dx.doi.org/10.1016/j.febslet.2012.05.003

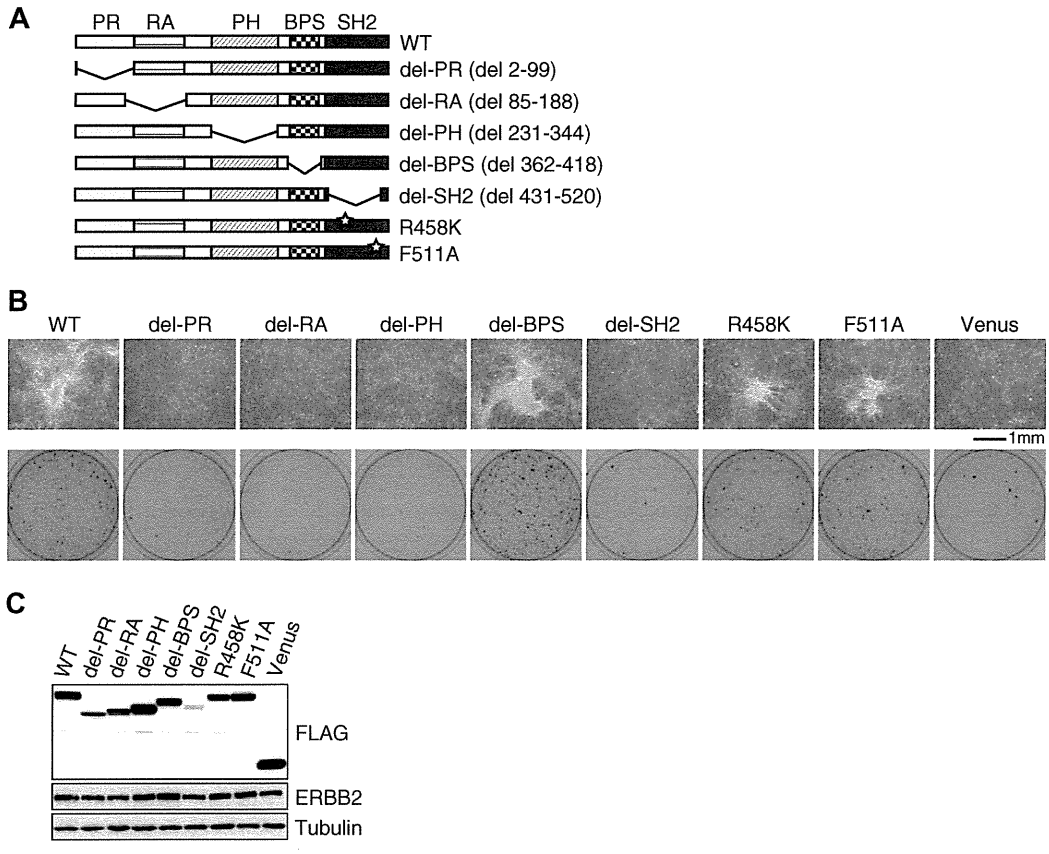

Fig. 3. Transforming activity of GRB7 domain deletion and point mutants. (A) Structures of the GRB7 mutants used in the experiments. (B) Focus formation assays with GRB7 mutants. 3T3-ERBB2 were infected with WT or mutant GRB7, and then cultured for 16 days (upper). Scale bar, 1 mm. Cells were fixed and stained with crystal violet (lower). (C) Expression level of ERBB2 and WT or mutant GRB7. Distinct amount of virus stock was used as follows: GRB7 WT (250 μl), del-PR (500 μl), del-RA (500 μl), del-PH (250 μl), del-BPS (250 μl), del-SH2 (500 μl), R458 K (500 μl), F511A (250 μl), Venus (250 μl).

pharose (GE Healthcare) for 1 h at 4 °C, then washed. Samples were boiled for 5 min in SDS–PAGE sample buffer, and separated with 7.5% or 10% acrylamide gels. Proteins were transferred onto PVDF membranes (Immobilon-P, Millipore), rinsed in TBS (20 mM Tris–HCl (pH 7.5), and 150 mM NaCl) and incubated in blocking buffer (TBS containing 3–5% non-fat dry milk or 5% bovine serum albumin) for 1 h at RT or overnight at 4 °C. The membranes were incubated for 1 h at RT or overnight at 4 °C with primary antibodies. Proteins were labeled using HRP-conjugated secondary antibodies diluted at 1:2000 for 1 h at RT, then visualized by the enhanced chemiluminescence method using Immobilon Western reagent (Millipore).

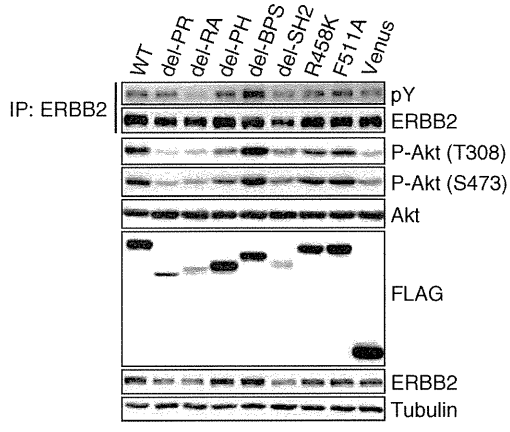

Fig. 4. Effect of GRB7 mutants on Akt phosphorylation. Lysates from 3T3-ERBB2, WT and mutant GRB7 were immunoblotted using anti-phospho-Akt-specific antibodies. ERBB2 immunoprecipitates were also analyzed to assess total phosphorylation by anti-phosphotyrosine antibody. Amounts of virus stock used are shown in Fig. 3.

3. Results

To screen for ERBB2-dependent transforming genes, we established NIH3T3 derivative (3T3-ERBB2) moderately expressing human WT ERBB2 under the control of CMV promoter. Mixtures of full-length human cDNA clones corresponding to the 52 genes (Table 1) within the *ERBB2* amplicon were cloned into pMX retroviral vectors, and then retroviral expression vectors were introduced into Plat-E packaging cells. 3T3-ERBB2 was infected with the resultant retrovirus mixture. Two to three weeks after infection, 30 foci were identified, whereas no foci were observed for 3T3-ERBB2 without retroviral infection. Each focus was isolated, expanded, and lysed for preparation of genomic DNA to analyze integrated cDNAs (Fig. 1A, Supplementary Table 1).

To test the transforming activity of most frequently recovered cDNAs, 12 representative cDNAs (Table 1) were individually introduced into 3T3-ERBB2. As a result, only GRB7 (RefSeq: NM_001030002) reproducibly induced foci. Transformed cells were smaller than normal cells and piled up on one another. The

Please cite this article in press as: Saito, M., et al. Expression screening of 17q12–21 amplicon reveals GRB7 as an ERBB2-dependent oncogene. FEBS Lett. (2012), http://dx.doi.org/10.1016/j.febslet.2012.05.003

Table 1
Fifty-two genes analyzed in this study.

Gene symbol	RefSeq ID	Frequency
C17orf78	**NM_173625**	**9**
TADA2A	NM_001166105	5
DUSP14	**NM_007026**	**9**
SYNRG	NM_001163546	0
DDX52	NM_007010	2
HNF1B	NM_000458	4
MRPL45	NM_032351	0
SOCS7	NM_014598	1
SRCIN1	NM_025248	0
MLLT6	NM_005937	0
PCGF2	NM_007144	5
PSMB3	NM_002795	3
PIP4K2B	NM_003559	0
CWC25	NM_017748	2
RPL23	NM_000978	6
LASP1	NM_006148	0
PLXDC1	NM_020405	4
CACNB1	NM_000723	3
RPL19	NM_000981	5
FBXL20	NM_032875	0
MED1	NM_004774	0
PPP1R1B	NM_032192	2
STARD3	**NM_001165937**	**11**
TCAP	**NM_003673**	**21**
PNMT	**NM_002686**	**11**
PGAP3	**NM_033419**	**16**
ERBB2	NM_004448	0
C17orf37	**NM_032339**	**7**
GRB7	**NM_001030002**	**11**
IKZF3	NM_012481	2
GSDMB	NM_001165959	0
ORMDL3	NM_139280	5
GSDMA	NM_178171	0
PSMD3	NM_002809	5
CSF3	**NM_172219**	**10**
MED24	NM_014815	1
THRA	**NM_001190919**	**7**
NR1D1	NM_021724	0
MSL1	NM_001012241	2
RAPGEFL1	NM_016339	2
WIPF2	NM_133264	0
CDC6	NM_001254	0
RARA	**NM_000964**	**9**
LOC100131821	AK123052	4
IGFBP4	NM_001552	6
TNS4	**NM_032865**	**13**
CCR7	NM_001838	2
SMARCE1	NM_003079	0
KRT24	NM_019016	2
KRT25	NM_181534	3
KRT28	NM_181535	3
TMEM99	NM_145274	0

Genes are aligned in order of chromosome location. Frequency of genes appeared in 30 foci are shown. 12 cDNAs individually introduced into 3T3-ERBB2 are shown in bold.

Table 2
Focus formation assay with GRB proteins and ERBB2.

	Number of foci after 20 days (10 cm-culture dish)				
	Venus	GRB2	GRB7	GRB10	GRB14
Experiment 1					
Control	0	0	0	0	0
ERBB2	0	2	6	0	0
Experiment 2					
Control	1	0	0	0	0
ERBB2	0	5	13	0	0

Distinct amount of virus stock were used as follows: Venus (30 μl), GRB2 (480 μl), GRB7 (90 μl), GRB10 (360 μl), GRB14 (480 μl) for control NIH3T3, and Venus (20 μl), GRB2 (360 μl), GRB7 (60 μl), GRB10 (240 μl), GRB14 (360 μl) for 3T3-ERBB2. Expression level of each protein was analyzed in Fig. 2C.

appearance of GRB7-transformed foci was smaller and higher than that of H-Ras(G12V)-transformed foci (data not shown). GRB7 induced transformation of 3T3-ERBB2, but not of parental NIH3T3 (Fig. 1B), indicating that transformation of NIH3T3 by GRB7 is dependent on ERBB2 expression.

GRB7 is one of the GRB7 family proteins, which are known to bind receptor tyrosine kinases and mediate signal to downstream effectors [13]. We carried out focus formation assays to determine whether ERBB2-dependent transforming activity is only limited to GRB7 or conserved in all GRB7 family proteins. We also tested GRB2, a well-known adaptor protein with distinct structure from GRB7, in addition to GRB7 family proteins. No foci were observed when each GRB protein (GRB2, GRB7, GRB10 and GRB14) was expressed individually in NIH3T3 cells; however, with the expression of ERBB2, a number of foci were reproducibly observed when either GRB7 or GRB2 was expressed (Fig. 2A, Table 2). This result indicates that ERBB2-dependent transforming activity was specific to GRB7 among the GRB7 family proteins.

To assess whether the transforming activity of GRB7 is based on activation of ERBB2, we evaluated the phosphorylation status of ERBB2 by expression of GRB7 compared with other GRB7 family proteins. To analyze total phosphorylation of ERBB2, whole cell lysates of 3T3-ERBB2 expressing one of the GRB7 family proteins were subjected to immunoprecipitation with an ERBB2 antibody. Then, the phosphorylation status of ERBB2 was analyzed using phosphotyrosine-specific antibody 4G10. As shown in Fig. 2B, ERBB2 phosphorylation was considerably upregulated in GRB7-expressing cells. GRB14 also increased ERBB2 phosphorylation; however, GRB10 had no effect. To determine which tyrosine residues of ERBB2 are phosphorylated when GRB7 is expressed, whole cell lysates of 3T3-ERBB2 expressing one of the GRB proteins were immunoblotted using a series of phospho-specific antibodies against ERBB2. As shown in Fig. 2C, phosphorylation of Tyr1221/1222 and Tyr1248 was upregulated in GRB7-expressing cells, while that of a Src phosphorylation site, Tyr877, was unaltered, suggesting that GRB7 promotes or retains ERBB2 autophosphorylation in particular. We therefore evaluated the effects of GRB7 and ERBB2 on signaling pathways that are frequently deregulated in cancer, that is, MAPK and PI3K-Akt pathways. We analyzed activation of components of these pathways by activation state-specific antibodies. These data showed that compared with other GRB proteins, co-expression of ERBB2 and GRB7 had no effect on the phosphorylation status of MEK or Erk. In contrast to components of the MAPK pathway, phosphorylation of Akt at Thr308 and Ser473 was marginally upregulated by expression of either ERBB2 or GRB7, but greatly upregulated when both proteins were expressed (Fig. 2C). These results suggest that cooperative transformation of ERBB2 and GRB7 may require Akt activation.

To dissect functional domains required for transforming activity of GRB7, we constructed five corresponding deletion mutants, PR (proline-rich), RA (Ras-associating), PH (Pleckstrin homology), BPS (between PH and SH2), and SH2 (Src-homology 2), and two point mutants for SH2 domain (Fig. 3A). R458K has a defect in the phosphotyrosine binding capacity of its SH2 domain, while F511A has a dimerization defect [14]. We assessed their transforming activity on 3T3-ERBB2 by focus formation assays. As shown in Fig. 3B and C, four GRB7 mutants, del-PR, del-RA, del-PH, and del-SH2, were defective in the transforming activity of 3T3-ERBB2 cells. R458K was also impaired in transforming activity, and the number of foci was reduced. In contrast, F511A retained comparable transforming activity with WT GRB7. However, del-BPS promoted foci formation, although its transforming activity was still dependent on ERBB2 (data not shown). Taken together, all four domains are required for ERBB2-dependent transforming activity of GRB7, except for its BPS region.

Please cite this article in press as: Saito, M., et al. Expression screening of 17q12–21 amplicon reveals GRB7 as an ERBB2-dependent oncogene. FEBS Lett. (2012), http://dx.doi.org/10.1016/j.febslet.2012.05.003

The BPS region of GRB7 family proteins is known to act as a pseudo substrate of the insulin and IGF1 receptors, and directly inhibits their catalytic activities [15]. Therefore, we hypothesized that BPS region of GRB7 downregulates ERBB2 kinase activity in spite of its activator function of ERBB2. To address this hypothesis, we compared WT and mutant GRB7 in terms of their effect on ERBB2 and Akt phosphorylation. As shown in Fig. 4, ERBB2 phosphorylation was increased by deletion of the BPS region. Moreover, Akt phosphorylation was concomitantly increased. These results indicate that the BPS region of GRB7 potentially represses ERBB2 activity in a similar manner to the inhibition of insulin and IGF1 receptors by GRB7 family proteins. Of the other transformation-deficient mutants, del-RA had no effect on ERBB2 and Akt phosphorylation, while del-PR, del-PH, and del-SH2 increased ERBB2 phosphorylation as well as WT but had no effect on Akt phosphorylation. Two point mutants with transforming activity retained ERBB2 and Akt phosphorylation. These results indicate that the transformed phenotype correlated with Akt activation status.

4. Discussion

Gene amplification is one of the major genetic alterations in cancer, which leads to overexpression of several genes. Amplicons recurrently observed in human cancers are likely to be positively selected owing to their contribution to oncogenesis, and indeed, amplicons have been shown to include cancer driver genes. But information on the significance of other co-amplified genes has been limited.

Accumulating clinical evidence indicate that *ERBB2* is a driver gene of several types of cancers. In fact, transforming activity of ERBB2 depends on its conformational status and expression level. An *ErbB2* mutant observed in rat neuroblastoma called *neu* oncogene, which tends to form dimers [16], has transforming activity [7]. Furthermore, strong expression of WT ERBB2 driven by retroviral LTR showed transforming activity [17]. In contrast, moderate expression of WT ERBB2 driven by SV40 promoter did not cause transformation [17]. We hypothesized that some of the genes in the 17q12–21 amplicon may cooperate with ERBB2 to cause tumorigenesis in the case ERBB2 expression is relatively low. To test this hypothesis, we assessed the transforming activity of all genes in the amplicon under the moderate expression of ERBB2. Our 3T3-ERBB2 cells formed neither foci nor colonies, enabling us to identify GRB7 as a gene that enhances the transforming activity of ERBB2.

In the screening of 52 genes in the amplicon, we detected integration of GRB7 in 11 out of 30 foci analyzed (Table 1, Supplementary Table 1). This result suggested the existence of oncogenes other than GRB7 in the amplicon. In fact, we identified another novel transforming gene in the amplicon with the same strategy using NMuMG-ERBB2, which we established by introducing ERBB2 expression vector into NMuMG, a mouse mammary epithelial cell line (A.M., manuscript in preparation). Some foci did not contain either of them (Supplementary Table 1). One possibility is that combination of multiple genes, which do not have independent transforming activity, causes transformation. Alternatively, recovering integrated cDNAs from genomic DNA of transformants may be biased in PCR amplification and cloning and thus some of the cDNAs might have been missed. Nevertheless, the fact that the remaining 50 genes (except for GRB7 and the novel transforming gene) in the *ERBB2* amplicon did not induce any foci strongly suggests that either of the two genes is necessary for cellular transformation.

GRB7 has a unique feature in the activation of ERBB2. ERBB2-dependent transforming activity is observed only in GRB7 among the GRB7 family proteins (Fig. 2A). Previous studies demonstrated GRB7 binds to ERBB family receptors, especially ERBB2 and ERBB3, through its SH2 domain [18]. Increased ERBB2 phosphorylation was observed in response to expression of GRB7, suggesting that this binding specificity contributes to its effect on ERBB2. Also in our transformation model, Akt phosphorylation correlated with the transformation phenotype of NIH3T3 (Figs. 3B and 4). Akt is deregulated in a wide spectrum of human cancers, such as breast, ovarian and thyroid cancers [19], and transforming activity of its truncated form in NIH3T3 has been reported [20]. Our results suggest activation of ERBB2-GRB7-Akt axis is sufficient for cellular transformation.

Our study with GRB7 mutants provides insights into the mechanism by which GRB7 activates ERBB2 and Akt. GRB7 family proteins consist of an RA domain, PH domain, BPS region and SH2 domain [13]. Among them, deletion of the BPS region in GRB7 increases ERBB2 phosphorylation and enhances transformation, suggesting two possibilities: first, the BPS region of GRB7 may inhibit ERBB2 kinase activities in a similar way that the BPS regions of GRB10 and GRB14 interfere with IGF1 receptors as pseudo-substrates [15]. Second, as it was recently shown that IGF1 receptor and ERBB2 were co-immunoprecipitated in SK-BR-3 breast cancer cells [21], GRB7 may enhance complex formation of ERBB2 and IGF1 receptor. If this is the case, lack of BPS region may facilitate IGF1 receptor to phosphorylate ERBB2. The RA domain, defined by sequence homology between the Ras effectors, is also involved in the phosphorylation of both ERBB2 and Akt. However, the molecular function of RA domain still remains to be elucidated.

Previous studies showed that GRB7 was required for SK-BR-3 cell proliferation and ERK1/2 and Akt phosphorylation [22,23]. Conversely, overexpression of GRB7 and ERBB2 in MCF-7 breast cancer cells enhance ERBB2 and Akt phosphorylation and tumor xenograft growth [24]. These studies suggested a possible involvement of GRB7 in the neoplastic phenotype of breast cancer cells. Beyond these studies, we further reveal GRB7 as a unique transforming gene, which does not show transforming activity by itself but cooperatively transforms NIH3T3 cells with ERBB2. Furthermore, we provide evidence for the significance of its BPS and RA domains in the ERBB2-GRB7-Akt signaling axis for cellular transformation.

Acknowledgments

We thank Kumiko Semba for her secretarial assistance. This research was partially supported by JSPS KAKENHI 23241064 and a grant for translational research programs from New Energy and Industrial Technology Development Organization (NEDO).

Appendix A. Supplementary data

Supplementary data associated with this article can be found, in the online version, at http://dx.doi.org/10.1016/j.febslet.2012.05.003.

References

[1] Santarius, T., Shipley, J., Brewer, D., Stratton, M.R. and Cooper, C.S. (2010) A census of amplified and overexpressed human cancer genes. Nat. Rev. Cancer 10, 59–64.
[2] Ito, E. et al. (2007) Novel clusters of highly expressed genes accompany genomic amplification in breast cancers. FEBS Lett. 581, 3909–3914.
[3] Hsu, D.S. et al. (2009) Characterizing the developmental pathways TTF-1, NKX2-8, and PAX9 in lung cancer. Proc. Natl. Acad. Sci. U S A 106, 5312–5317.
[4] Kauraniemi, P. and Kallioniemi, A. (2006) Activation of multiple cancer-associated genes at the ERBB2 amplicon in breast cancer. Endocr. Relat. Cancer 13, 39–49.

Please cite this article in press as: Saito, M., et al. Expression screening of 17q12–21 amplicon reveals GRB7 as an ERBB2-dependent oncogene. FEBS Lett. (2012), http://dx.doi.org/10.1016/j.febslet.2012.05.003

[5] Yamamoto, T. et al. (2011) ErbB2/HER2: its Contribution to Basic Cancer Biology and the Development of Molecular Targeted Therapy in: Breast Cancer – Carcinogenesis, Cell Growth and Signalling Pathways (Gunduz, M., Ed.), InTech, Rijeka, Croatia.
[6] Slamon, D.J., Clark, G.M., Wong, S.G., Levin, W.J., Ullrich, A. and McGuire, W.L. (1987) Human breast cancer: correlation of relapse and survival with amplification of the HER-2/neu oncogene. Science 235, 177–182.
[7] Bargmann, C.I., Hung, M.C. and Weinberg, R.A. (1986) Multiple independent activations of the neu oncogene by a point mutation altering the transmembrane domain of p185. Cell 45, 649–657.
[8] Muller, W.J., Sinn, E., Pattengale, P.K., Wallace, R. and Leder, P. (1988) Single-step induction of mammary adenocarcinoma in transgenic mice bearing the activated c-neu oncogene. Cell 54, 105–115.
[9] Goshima, N. et al. (2008) Human protein factory for converting the transcriptome into an in vitro-expressed proteome. Nat. Methods 5, 1011–1017.
[10] Kitamura, T., Koshino, Y., Shibata, F., Oki, T., Nakajima, H., Nosaka, T. and Kumagai, H. (2003) Retrovirus-mediated gene transfer and expression cloning: powerful tools in functional genomics. Exp. Hematol. 31, 1007–1014.
[11] Nagai, T., Ibata, K., Park, E.S., Kubota, M., Mikoshiba, K. and Miyawaki, A. (2002) A variant of yellow fluorescent protein with fast and efficient maturation for cell-biological applications. Nat. Biotechnol. 20, 87–90.
[12] Rabhi, I., Guedel, N., Chouk, I., Zerria, K., Barbouche, M.R., Dellagi, K. and Fathallah, D.M. (2004) A novel simple and rapid PCR-based site-directed mutagenesis method. Mol. Biotechnol. 26, 27–34.
[13] Han, D.C., Shen, T.L. and Guan, J.L. (2001) The Grb7 family proteins: structure, interactions with other signaling molecules and potential cellular functions. Oncogene 20, 6315–6321.
[14] Porter, C.J., Wilce, M.C., Mackay, J.P., Leedman, P. and Wilce, J.A. (2005) Grb7-SH2 domain dimerisation is affected by a single point mutation. Eur. Biophys. J. 34, 454–460.
[15] Stein, E.G., Gustafson, T.A. and Hubbard, S.R. (2001) The BPS domain of Grb10 inhibits the catalytic activity of the insulin and IGF1 receptors. FEBS Lett. 493, 106–111.
[16] Weiner, D.B., Liu, J., Cohen, J.A., Williams, W.V. and Greene, M.I. (1989) A point mutation in the neu oncogene mimics ligand induction of receptor aggregation. Nature 339, 230–231.
[17] Di Fiore, P.P., Pierce, J.H., Kraus, M.H., Segatto, O., King, C.R. and Aaronson, S.A. (1987) ErbB-2 is a potent oncogene when overexpressed in NIH/3T3 cells. Science 237, 178–182.
[18] Stein, D. et al. (1994) The SH2 domain protein GRB-7 is co-amplified, overexpressed and in a tight complex with HER2 in breast cancer. EMBO J. 13, 1331–1340.
[19] Vivanco, I. and Sawyers, C.L. (2002) The phosphatidylinositol 3-Kinase AKT pathway in human cancer. Nat. Rev. Cancer 2, 489–501.
[20] Cheng, J.Q., Altomare, D.A., Klein, M.A., Lee, W.C., Kruh, G.D., Lissy, N.A. and Testa, J.R. (1997) Transforming activity and mitosis-related expression of the AKT2 oncogene: evidence suggesting a link between cell cycle regulation and oncogenesis. Oncogene 14, 2793–2801.
[21] Nahta, R., Yuan, L.X., Zhang, B., Kobayashi, R. and Esteva, F.J. (2005) Insulin-like growth factor-I receptor/human epidermal growth factor receptor 2 heterodimerization contributes to trastuzumab resistance of breast cancer cells. Cancer Res. 65, 11118–11128.
[22] Chu, P.Y., Li, T.K., Ding, S.T., Lai, I.R. and Shen, T.L. (2010) EGF-induced Grb7 recruits and promotes Ras activity essential for the tumorigenicity of Sk-Br3 breast cancer cells. J. Biol. Chem. 285, 29279–29285.
[23] Nencioni, A. et al. (2010) Grb7 upregulation is a molecular adaptation to HER2 signaling inhibition due to removal of Akt-mediated gene repression. PLoS One 5, e9024.
[24] Bai, T. and Luoh, S.W. (2008) GRB-7 facilitates HER-2/Neu-mediated signal transduction and tumor formation. Carcinogenesis 29, 473–479.

Please cite this article in press as: Saito, M., et al. Expression screening of 17q12–21 amplicon reveals GRB7 as an ERBB2-dependent oncogene. FEBS Lett. (2012), http://dx.doi.org/10.1016/j.febslet.2012.05.003

Alternative 3'-end processing of nuclear-retained long noncoding RNAs initiates construction of nuclear paraspeckles with multiple RNA-binding proteins

Takao Naganuma[1], Shinichi Nakagawa[3], Akie Tanigawa[1], Yasnory F Sasaki[1], Naoki Goshima[2], and Tetsuro Hirose[1,*]

[1]Functional RNomics Team and [2]Biological Systems Control Team, Biomedicinal Information Research Center, National Institute of Advanced Industrial Science and Technology (AIST), 2-4-7 Aomi, Koutou, Tokyo 135-0064, Japan

[3]RNA Biology Laboratory, RIKEN Advanced Science Institute, 2-1 Hirosawa, Wako, 351-0198, Japan

*Address correspondence to: tets-hirose@aist.go.jp

Running title: LncRNA processing for nuclear body architecture

Summary

Paraspeckles are unique subnuclear structures built on specific long noncoding RNAs (MENε/β). The MENε and MENβ isoforms arise from alternative 3'-end processing. This study defined MENβ, but not MENε, as an essential RNA component for de novo paraspeckle formation, by plasmid rescue into MEFs from MENε/β knockout mice. Thirty-five paraspeckle proteins (PSPs) were mainly identified by the colocalization of human proteins expressed from full-length cDNAs. RNAi analyses identified seven PSPs that were essential for paraspeckle formation. Only four of these PSPs were indispensible for MENβ accumulation, which indicated that MENβ accumulation is indispensible but insufficient for paraspeckle formation. Alternative 3'-end processing of MENε/β involved hnRNP K, which was required for MENβ accumulation. By capturing CFIm25 from the functional CFIm, hnRNP K arrested the RNA-binding of CFIm that was required for the 3'-end processing of MENε. This step led to the preferential accumulation of MENβ and initiated paraspeckle construction with multiple PSPs.

INTRODUCTION

Recent postgenomic transcriptome analyses have revealed that many nonprotein coding transcripts, so-called noncoding RNAs (ncRNAs), are transcribed from large portions of mammalian genomes (Carninci et al., 2005; Kapranov et al., 2007). The limited numbers of long ncRNAs that have been characterized exhibit diverse functions, as well as cell type-specific expression and localization to subcellular compartments (Prasanth and Spector, 2007;

Mercer et al., 2009; Wang and Chang, 2011). Most of the newly discovered ncRNAs are likely transcribed by RNA polymerase II. However, extensive analysis of the subcellular localization of human transcripts reveals that ncRNAs are enriched in the cell nucleus, suggesting that they play diverse roles in nuclear events (Prasanth and Spector 2007; Kapranov et al., 2007).

The mammalian cell nucleus is highly organized. It is composed of distinct nuclear bodies that contain proteins or RNAs characteristic of particular nuclear processes. To date, approximately 10 different nuclear bodies have been characterized (Spector, 2006). Several long ncRNAs, such as Xist, Gomafu (Miat), Malat1 (NEAT2), MENε/β (NEAT1_v1/NEAT1_v2), TUG1 and GRC-RNAs, localize to specific nuclear bodies (Clemson et al., 1996, 2009; Hutchinson et al., 2007; Sasaki et al., 2009; Sone et al., 2007; Sunwoo et al., 2009; Yang et al., 2011; Zheng et al. 2010). In particular, Malat1 localizes to nuclear speckles, where it regulates alternative splicing by modulating the phosphorylation status of Serine/Arginine (SR)-splicing factors (Tripathi et al., 2010). Malat1 controls growth signal-responsive gene expression through association of unmethylated polycomb 2 protein (Yang et al., 2011).

Paraspeckles are recently discovered nuclear bodies that are usually detected in cultured cell lines as a variable number of foci found in close proximity to the nuclear speckles. Paraspeckles contain characteristic RNA-binding proteins, including paraspeckle protein 1 (PSP1), PSP2, p54nrb, CFIm68, and PSF (Fox et al., 2002; Dettwiler et al., 2004; Prasanth et al., 2005). PSP1, p54nrb, and PSF share common domain structures comprised of two RNA-recognition motifs (RRMs). Collectively, these three proteins comprise

the *Drosophila melanogaster* behavior and human splicing (DBHS) protein family (Bond and Fox, 2009).

The discovery of the specific paraspeckle localization of MENε/β ncRNAs opened a new window in paraspeckle research (Chen and Carmichael, 2009; Clemson et al., 2009; Sasaki et al., 2009; Sunwoo et al., 2009). MENε/β ncRNAs are transcribed from a genetic locus called familial tumor syndrome multiple endocrine neoplasia (MEN) type I on human chromosome 11 (Guru et al., 1997) and are comprised of two isoform transcripts, 3.7-kb MENε and 23-kb MENβ. Both RNAs are produced from the same promoter. Alternatively, they can be processed at the 3'-end to produce a canonically polyadenylated MENε and a noncanonically processed MENβ. RNase P recognizes the tRNA-like structure and cleaves it to form the nonpolyadenylated 3'-end of MENβ (Sunwoo et al., 2009). The knockdown of MENε/β ncRNAs leads to the disintegration of paraspeckles, suggesting that these ncRNAs serve as a core structural component (Chen and Carmichael, 2009; Clemson et al., 2009; Sasaki et al., 2009; Sunwoo et al., 2009). However, the biological function of paraspeckles and the role(s) of MENε/β ncRNAs remain to be elucidated.

We recently found that paraspeckles were not essential for viability and development in a mouse model under normal conditions, suggesting that they play roles under certain stress conditions (Nakagawa et al., 2011). It has been noted that CTN-RNA, an isoform of mCat2 mRNA, is retained specifically in the paraspeckle. Intriguingly, the long 3' untranslated region (UTR) of CTN-RNA is cleaved by an unidentified endoribonuclease upon exposure to certain stresses, which leads to the export of processed mCat2 mRNA for cytoplasmic translation

(Parasanth et al., 2005). The CTN-RNA 3' UTR contains a long inverted-repeat sequence that is capable of forming intramolecular double-stranded RNAs that are A-to-I edited. The hyperedited CTN-RNAs are enriched in the paraspeckles. Thus, paraspeckles are thought to suppress the expression of hyperedited transcripts through nuclear retention (Prasanth et al., 2005). Inverted Alu repeat sequences are commonly found in the 3' UTRs of multiple mRNAs in human cells (Chen et al., 2008). This finding suggests that the expression of these transcripts is suppressed by a nuclear retention mechanism.

We previously reported that two paraspeckle-localized DBHS family proteins, PSF and p54nrb, are required for paraspeckle integrity and for the accumulation of MENβ but not MENε (Sasaki et al., 2009). These results suggest that MENε alone is unable to maintain paraspeckle integrity. By contrast, overexpressed MENε reportedly is capable of increasing the number of paraspeckles, which suggests that it is the functional isoform for paraspeckle formation (Clemson et al., 2009). An electron microscopic study revealed the location of the MENβ and MENε isoforms. The common MENε/β region and MENβ 3'-terminal region were located at the paraspeckle periphery, whereas the MENβ middle region was located in the paraspeckle interior. These findings suggest the importance of MENβ for the maintenance of paraspeckle integrity (Souquere et al., 2010).

In this study, the essential components for paraspeckle formation were determined. Plasmid rescue experiments revealed that MENβ, but not MENε, is a necessary RNA for de novo paraspeckle formation. To analyze the detailed process of paraspeckle formation, we sought to identify unknown paraspeckle

components. RNAi analyses identified additional factors, each with distinct roles, which were indispensible for paraspeckle formation. One of the essential PSPs was involved in the alternative 3'-end processing of MENε/β. This protein arrested the canonical MENε 3'-end processing, which led to preferential selection for the noncanonical processing of the MENβ 3'-end. Our data provide important insights into the process of paraspeckle formation on the specific nuclear-retained long ncRNAs.

RESULTS

The MENβ ncRNA isoform is essential for paraspeckle formation

We first attempted to clarify which MENε/β isoform(s) were required for de novo paraspeckle formation. MEFs were prepared from MENε/β knockout mice (MEF-/-) (Nakagawa et al., 2011), in which paraspeckles were absent, for rescue experiments with the expression plasmid of either the MENε or MENβ isoform. Many of the paraspeckle-like foci that were detectable with both anti-PSF antibody immunostaining and MENε/β RNA-FISH appeared when MENβ but not MENε was transiently expressed from the plasmid (Figures 1A, S1A and S1B). This result indicates that MENβ is an authentic RNA component that is capable of de novo paraspeckle formation.

To prove that the rescued foci exhibited characteristics common to endogenous paraspeckles, the transfected MEF(-/-) were treated with actinomycin D. Rescued foci did not appear with actinomycin D treatment. Instead, PSF-Flag (as a cotransfected marker) and endogenous PSPs relocated to perinucleolar caps, from which MENβ ncRNA was absent (Figure

1B). Paraspeckles reportedly display actinomycin D-induced disruption and the concomitant relocation of protein components (Fox et al., 2002; Shav-Tal et al., 2005). In the present study, the overexpression of either MENβ or MENε in NIH3T3 cells led to elevated nuclear paraspeckle numbers; however, MENβ was more stimulatory than MENε (Figures 1C and S1C). Taken together, these results indicate that the MENβ isoform is an essential RNA component for paraspeckle formation.

Identification of new paraspeckle components

We previously reported that two RNA-binding proteins that are essential for paraspeckle formation, p54nrb and PSF, preferentially bind to and stabilize the MENβ isoform (Sasaki et al., 2009). To obtain further insights into the paraspeckle structure, additional PSPs were searched for by employing the human full-length cDNA resource (FLJ Clones) available from the authors' affiliate (Maruyama et al., 2009). In this cDNA collection, the intact protein-coding regions of 18,467 human proteins are fused with Venus fluorescent protein. FLJ Clones provides information concerning the intracellular localization of >18,000 human proteins, through the transfection of each cDNA clone (Figure 2A).

Initially, 68 cDNA clones whose products exhibited the typical localization pattern of paraspeckle-like nuclear foci were selected. The identities of the foci were determined by immunostaining the endogenous PSF, to see if the Venus signals overlapped with the PSF signals (Figures 2B and S2A and Table S1) but not the signals of other nuclear bodies (Figure S3B). This screening led to the

eventual selection of 34 cDNA clones. Endogenous proteins corresponding to the identified cDNA clones were immunostained with their respective antibodies, when available (Figures 2C and S2B and Table S1). The correct paraspeckle localization of all 27 examined proteins was confirmed, and no false positives were identified.

As a second screen, we confirmed the relocation of each Venus-fusion protein upon actinomycin D treatment (Figure 1B). All 34 fusion proteins relocated to the perinucleolar caps (Table S1). These caps corresponded to the destination of the endogenous PSPs (Figures 2D and S3A), but were distinct from those of the nucleolar or Cajal body proteins (Figure S3B).

Therefore, 34 cDNA clones, designated PSP3-PSP36, were confirmed as new PSPs. Additionally, TDP43, which was recently reported to interact prominently with MENε/β ncRNAs in the brain from frontotemporal lobar degeneration (FTLD) patients (Tollervey et al., 2011), was confirmed to localize to the paraspeckle in HeLa cells by immunostaining of endogenous protein (Figure S2B). A comparison of all of the PSPs (Table 1 and Figure S4) indicated that most possessed canonical RNA-binding domains (Burd and Dreyfuss, 1994): 20 proteins with RRMs, two proteins with KH motifs, and five proteins with RGG boxes. Eight proteins possessed one or more zinc finger motifs, which are involved in RNA-binding (Brown 2005). Although the numbers are limited, some PSPs possessed putative DNA-binding domains, including the AT-hook, Zn finger, homeodomain, and SAP domain.

Functional assignments for each PSP identified additional essential factors for paraspeckle formation

To investigate the respective roles of the newly identified and known PSPs in paraspeckle construction, each PSP was knocked-down with at least two independent siRNAs (Table S2). The resultant changes in paraspeckle appearance [i.e., proportion (%) of cells possessing intact paraspeckles] and in the levels of each MENε/β isoform (summarized in Table S3) were examined.

The PSPs were classified into three distinct categories according to the proportion of paraspeckle-possessing cells after RNAi. After treatment with control siRNA, 88% of the cells examined possessed paraspeckles; this group was defined as the control (Ctl) group (100%). Categories 1, 2, and 3 included PSPs whose RNAi led to a marked decrease (≤30% of Ctl), substantial decrease (30–75% of Ctl), or no obvious change (≤75% of Ctl) in the proportion of paraspeckle-possessing cells, respectively (Table S3 and Figure S5). Investigation of the MENε/β levels by RNase protection assays (RPAs) revealed that category 1 could be divided into two subcategories, in which the MENβ levels were markedly diminished to ≤30% (category 1A) or were unchanged (category 1B). Similarly, category 3 was divided into two subcategories, in which MENε levels were either diminished to ≤30% (category 3A) or were unchanged (category 3B). The PSP categorization is summarized in Tables 1 and S3 and Figure S5. Representative data from each of the five categories are shown in Figure 3C–3G.

Several PSPs were unable to be categorized because their expression was either undetectable in HeLa cells (PSP5, 9, and 23) or they showed